Statistical uncertainty in estimates of an effective scatterer number density for ultrasound

Jian-Feng Chen
Department of Medical Physics, University of Wisconsin, Madison, Wisconsin 53706

James A. Zagzebski
Departments of Medical Physics, Radiology, and Human Oncology, University of Wisconsin, Madison, Wisconsin 53706

Ernest L. Madsen
Department of Medical Physics, University of Wisconsin, Madison, Wisconsin 53706

(Received 23 October 1993; revised 12 May 1994; accepted 25 May 1994)

In a previous paper [J. Acoust. Soc. Am. **95**, 77–85 (1994)], a method for determining *an effective scatterer number density* in ultrasonography was presented. This is the actual number density multiplied by a frequency-dependent factor that depends on the differential scattering cross sections of all scatterers. This method involves evaluating the ratio of the fourth moment to the square of the second moment of echo signals scattered from the sample. The random processes involved in forming these echo signals give rise to an uncertainty in the estimated effective scatterer number density. This uncertainty is evaluated here using error propagation. The statistical uncertainty depends on the effective number of scatterers contributing to the segmented echo signal; it increases when the effective number of scatterers increases. Tests of the statistical uncertainty estimator were in good agreement with uncertainties computed from experimental data.

PACS numbers: 43.20.Gp, 43.20.Jr, 43.80.Cs, 43.80.Vj

INTRODUCTION

In an earlier paper we described a method for determining an effective scatterer number density in ultrasound backscatter experiments.[1] This method involves evaluating the ratio of the fourth moment to the square of the second moment of the Fourier transform of the backscattered echo signal. The effective scatterer number density is found after applying data reduction algorithms that account for experimental factors in this ratio. Tests in phantoms having scatterer concentrations ranging from 134 to 750 cm^{-3} indicate the method yields accurate results in an *in vitro* experimental setup.[1]

This paper is concerned with uncertainties in estimates of the effective scatterer number density. In general, there are two categories of uncertainties present.[2] One is methodological and instrumental, due, for example, to instrumental inaccuracy and electronic noise. Another is statistical due to the random processes involved in forming the echo signals. The purpose of this paper is to determine the statistical uncertainty due to these latter, random processes.

Previously, Sleefe and Lele,[3,4] Wilhelmij and Denbigh,[5] and Denbigh and Smith[6] evaluated higher moments of backscattered signals, computed scatterer number densities and estimated statistical uncertainties. A methodology similar to that of these authors is employed in our work in computing the number density. However, our approach differs from these earlier methods in that it retains frequency dependent factors in the medium's scattering properties, yielding a frequency dependent, "effective scatterer number density" as the outcome of the estimate. In addition, expressions for the transducer field and for a gating function applied to select echo signals from a region of interest are retained in the analysis, avoiding the use of arbitrary limits of the field when defining the scattering volume. The advantage of this more thorough treatment is the fact that the effect of experimental parameters on the statistical uncertainty, such as the properties of the transducer, the transmitted pulse bandwidth and the gate duration, can readily be studied by modeling.

I. THEORY

A. Method for determining scatterer number density

The data reduction method for measuring the effective scatterer number density has been described previously,[1] so it will be outlined only briefly here. We consider the situation where a pulsed transducer is used to insonify a medium containing scatterers (see Fig. 1). The same transducer serves as a receiver for echoes scattered from the medium. Randomly distributed discrete scatterers are assumed to give rise to all echoes, and over the surface of the transducer, the scattered wave from each is assumed to be spherically symmetric about the position of the scatterer. Because of the random distribution of scatterers, the echo signal $V(t)$, or its gated Fourier transform $V_g(\omega)$, is a random variable. The latter quantity is modeled by[1]

$$V_g(\omega)=\int_{-\infty}^{+\infty} d\omega'\; T(\omega')B_0(\omega')W(\omega-\omega') \times\sum_{i=1}^{M}\psi_i(\omega')A^2(\mathbf{r}_i,\omega'), \tag{1}$$

where $T(\omega)$ is a complex transfer function relating the net instantaneous force on the transducer at the angular fre-

 0001-4966/94/96(4)/2556/8/$6.00

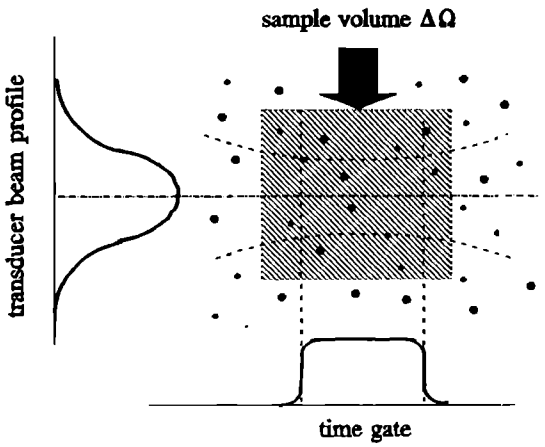

FIG. 1. A volume $\Delta\Omega$ in the medium containing M scatterers. The volume is wide enough compared to the ultrasound beam and extends a sufficient distance axially to include all scatterers contributing to the gated echo signal segment, described in Eq. (1).

quency ω to the detected voltage. $B_0(\omega)$ is a complex superposition coefficient corresponding to the frequency composition of the emitted pulse. $\psi_i(\omega)$ is the value of the angular distribution factor[7] at a 180° scattering angle for the ith scatterer at position $\mathbf{r}_i$. The sum is over all scatterers, M, in the sample volume, $\Delta\Omega$. This volume is wide enough compared to the ultrasound beam, expressed as $A(\mathbf{r},\omega)$, and extends a sufficient distance axially to include all scatterers contributing to any significant degree to the gated echo signal segment. $W(\omega-\omega')$ is the Fourier transform of the gating function.

When the number of scatterers, M, follows the Poisson distribution, and for gate durations that are long compared to the period of the wave, the ratio of the fourth moment to the square of the second moment of the frequency domain echo signal is given by[1]

$$\frac{\langle (V_g(\omega)V_g^*(\omega))^2\rangle}{\langle V_g(\omega)V_g^*(\omega)\rangle^2} = 2+\frac{1}{N_{\text{eff}}(\omega)}\frac{\iiint_{\Delta\Omega} d\mathbf{r}\|J(\mathbf{r},\omega)\|^4}{\{\iiint_{\Delta\Omega} d\mathbf{r}\|J(\mathbf{r},\omega)\|^2\}^2}, \tag{2}$$

where $\langle\cdots\rangle$ stands for the expectation value, and

$$N_{\text{eff}}(\omega)\equiv\langle N\rangle\frac{\langle\|\psi(\omega)\|^2\rangle^2}{\langle\|\psi(\omega)\|^4\rangle} \tag{3}$$

is the "effective scatterer number density" at angular frequency ω. This quantity is the actual mean number density $\langle N\rangle$ multiplied by a frequency-dependent factor $\langle\|\psi(\omega)\|^2\rangle^2/\langle\|\psi(\omega)\|^4\rangle$. The latter quantity depends on $\|\psi(\omega)\|^2=\psi(\omega)\psi^*(\omega)$, which is the differential scattering cross section for each scatterer at frequency ω and a scattering angle of 180°.[6] The quantity $J(\mathbf{r},\omega)$ is given by

$$J(\mathbf{r},\omega)\equiv\int_{-\infty}^{\infty} d\omega' T(\omega')B_0(\omega')W(\omega-\omega')A^2(\mathbf{r},\omega'), \tag{4}$$

where the factors in the integrand are defined above. Equation (2) is similar to that derived by Jakeman,[8] but differs in that here the experimental conditions including the transducer field and the effects of the signal segmenting time gate are explicitly accounted for. If we define

$$Y(\omega)\equiv\frac{\langle (V_g(\omega)V_g^*(\omega))^2\rangle}{\langle V_g(\omega)V_g^*(\omega)\rangle^2}-2,$$

Eq. (2) can be simplified to

$$N_{\text{eff}}(\omega)=Y(\omega)^{-1}\times\frac{\iiint_{\Delta\Omega} d\mathbf{r}\|J(\mathbf{r},\omega)\|^4}{\{\iiint_{\Delta\Omega} d\mathbf{r}\|J(\mathbf{r},\omega)\|^2\}^2}. \tag{5}$$

B. Error analysis

In an actual measurement, one computes

$$\Lambda(\omega)\equiv\frac{J_n(\omega)}{I_n^2(\omega)}-2$$

instead of $Y(\omega)$. Here $I_n(\omega)$ and $J_n(\omega)$ are the experimental sample means of the random variables $i(\omega)\equiv V_g(\omega)V_g^*(\omega)$ and $i^2(\omega)\equiv[V_g(\omega)V_g^*(\omega)]^2$ for n independent echo signal waveforms. The variances of $I_n(\omega)$ and $J_n(\omega)$ are given by $\sigma_I^2=\sigma_i^2/n$ and $\sigma_J^2=\sigma_j^2/n$, where σ_i^2 and σ_j^2 are the variances of $i(\omega)$ and $i^2(\omega)$, given by $\sigma_i^2=\langle i^2(\omega)\rangle-\langle i(\omega)\rangle^2$ and $\sigma_j^2=\langle i^4(\omega)\rangle-\langle i^2(\omega)\rangle^2$, respectively.

The variance of the variable $\Lambda(\omega)$ is given by[9]

$$\sigma_\Lambda^2=\left(\frac{\partial\Lambda(\omega)}{\partial I_n(\omega)}\right)^2\sigma_J^2+\left(\frac{\partial\Lambda(\omega)}{\partial I_n(\omega)}\right)^2\sigma_I^2+2\left(\frac{\partial\Lambda(\omega)}{\partial I_n(\omega)}\times\frac{\partial\Lambda(\omega)}{\partial J_n(\omega)}\right)\sigma_{IJ}^2$$

$$=\frac{1}{I_n^4(\omega)}\sigma_J^2+4\frac{J_n^2(\omega)}{I_n^6(\omega)}\sigma_I^2-4\frac{J_n(\omega)}{I_n^5(\omega)}\sigma_{IJ}^2$$

$$=\frac{1}{n}\left\{\frac{1}{I_n^4(\omega)}\sigma_j^2+4\frac{J_n^2(\omega)}{I_n^6(\omega)}\sigma_i^2-4\frac{J_n(\omega)}{I_n^5(\omega)}\sigma_{ij}^2\right\}, \tag{6}$$

where σ_{ij}^2 is the covariance of random variables $i(\omega)-\langle i(\omega)\rangle$ and $i^2(\omega)-\langle i^2(\omega)\rangle$. This is given by

$$\sigma_{ij}^2=\langle(i^2(\omega)-\langle i^2(\omega)\rangle)\cdot(i(\omega)-\langle i(\omega)\rangle)\rangle$$
$$=\langle i^3(\omega)\rangle-\langle i^2(\omega)\rangle\langle i(\omega)\rangle.$$

If n is large enough, we have, $I_n(\omega)\simeq\langle i(\omega)\rangle$, and $J_n(\omega)\simeq\langle i^2(\omega)\rangle$. In that case, Eq. (6) can be simplified to:

$$\sigma_\Lambda^2\simeq\frac{1}{n}\left\{\frac{L_n(\omega)}{I_n^4(\omega)}-\frac{J_n^2(\omega)}{I_n^4(\omega)}+4\frac{J_n^3(\omega)}{I_n^6(\omega)}-4\frac{J_n(\omega)K_n(\omega)}{I_n^5(\omega)}\right\}, \tag{7}$$

where $K_n(\omega)$ and $L_n(\omega)$ are the experimental sample means of $i^3(\omega)$ and $i^4(\omega)$.

The independent waveforms are recorded by translating the transducer, and hence the sample volume, $\Delta\Omega$, with respect to the sample. Because the number of scatterers, M, is assumed to follow the Poisson distribution, we have,

$$\sum_{M=0}^{+\infty} P(M)M=\langle M\rangle,$$

and

$$\sum_{M=0}^{+\infty} P(M)M(M-1)=\langle M\rangle^2,$$

and so forth, where $P(M)$ is the probability density function for the Poisson distribution. Therefore, we have[1,6]

$$I_n(\omega)\approx\langle i(\omega)\rangle = \langle N\rangle\langle\|\psi(\omega)\|^2\rangle\iiint_{\Delta\Omega} d\mathbf{r}\|J(\mathbf{r},\omega)\|^2,$$

and

$$J_n(\omega)\approx\langle i^2(\omega)\rangle = 2\langle N\rangle^2\langle\|\psi(\omega)\|^2\rangle^2\left\{\iiint_{\Delta\Omega} d\mathbf{r}\|J(\mathbf{r},\omega)\|^2\right\}^2 + \langle N\rangle\langle\|\psi(\omega)\|^4\rangle\iiint_{\Delta\Omega} d\mathbf{r}\|J(\mathbf{r},\omega)\|^4,$$

where we have substituted $\langle N\rangle=\langle M\rangle/\Delta\Omega$.

Using the same analysis techniques, we have

$$K_n(\omega)\approx\langle i^3(\omega)\rangle = 6\langle N\rangle^3\langle\|\psi(\omega)\|^2\rangle^3\left\{\iiint_{\Delta\Omega} d\mathbf{r}\|J(\mathbf{r},\omega)\|^2\right\}^2 + 9\langle N\rangle^2\langle\|\psi(\omega)\|^2\rangle\langle\|\psi(\omega)\|^4\rangle\iiint_{\Delta\Omega} d\mathbf{r}\|J(\mathbf{r},\omega)\|^2 \times\iiint_{\Delta\Omega} d\mathbf{r}\|J(\mathbf{r},\omega)\|^4 + \langle N\rangle\langle\|\psi(\omega)\|^6\rangle\iiint_{\Delta\Omega} d\mathbf{r}\|J(\mathbf{r},\omega)\|^6$$

and

$$\begin{aligned}L_n(\omega)\approx\langle i^4(\omega)\rangle = {} & 24\langle N\rangle^4\langle\|\psi(\omega)\|^2\rangle^4\left\{\iiint_{\Delta\Omega} d\mathbf{r}\|J(\mathbf{r},\omega)\|^2\right\}^4 + 72\langle N\rangle^3\langle\|\psi(\omega)\|^2\rangle^2\langle\|\psi(\omega)\|^4\rangle \\ & \times\left\{\iiint_{\Delta\Omega} d\mathbf{r}\|J(\mathbf{r},\omega)\|^2\right\}^2\iiint_{\Delta\Omega} d\mathbf{r}\|J(\mathbf{r},\omega)\|^4 + 18\langle N\rangle^2\langle\|\psi(\omega)\|^4\rangle^2\left\{\iiint_{\Delta\Omega} d\mathbf{r}\|J(\mathbf{r},\omega)\|^4\right\}^2 \\ & + 16\langle N\rangle^2\langle\|\psi(\omega)\|^2\rangle\langle\|\psi(\omega)\|^6\rangle\iiint_{\Delta\Omega} d\mathbf{r}\|J(\mathbf{r},\omega)\|^2\iiint_{\Delta\Omega} d\mathbf{r}\|J(\mathbf{r},\omega)\|^6 \\ & + \langle N\rangle\langle\|\psi(\omega)\|^8\rangle\iiint_{\Delta\Omega} d\mathbf{r}\|J(\mathbf{r},\omega)\|^8.\end{aligned}$$

We define the average "effective number" of scatterers contributing to the echo signal, M_{eff} as

$$M_{\text{eff}}(\omega)\equiv N_{\text{eff}}(\omega)V_{\text{eff}}(\omega), \tag{8}$$

where $N_{\text{eff}}(\omega)$ is the effective scatterer number density and the ratio of the volume integrals

$$V_{\text{eff}}(\omega)\equiv\frac{\{\iiint_{\Delta\Omega} d\mathbf{r}\|J(\mathbf{r},\omega)\|^2\}^2}{\iiint_{\Delta\Omega} d\mathbf{r}\|J(\mathbf{r},\omega)\|^4} \tag{9}$$

is defined to be an effective sample volume for this analysis. The ratios of the various higher moments in Eq. (7) are thus given by

$$\frac{J_n(\omega)}{I_n^2(\omega)}\approx 2+\frac{1}{M_{\text{eff}}(\omega)}, \tag{10}$$

$$\frac{K_n(\omega)}{I_n^3(\omega)}\approx 6+\frac{9}{M_{\text{eff}}(\omega)}+\frac{a_1(\omega)b_1(\omega)}{M_{\text{eff}}^2(\omega)}, \tag{11}$$

and

$$\frac{L_n(\omega)}{I_n^4(\omega)}\approx 24+\frac{72}{M_{\text{eff}}(\omega)}+\frac{18}{M_{\text{eff}}^2(\omega)}+\frac{16a_1(\omega)b_1(\omega)}{M_{\text{eff}}^2(\omega)}+\frac{a_2(\omega)b_2(\omega)}{M_{\text{eff}}^3(\omega)}, \tag{12}$$

where $a_1(\omega)$ and $a_2(\omega)$ are frequency-dependent coefficients related to the medium. These are given by

$$a_1(\omega)\equiv\frac{\langle\|\psi(\omega)\|^2\rangle\langle\|\psi(\omega)\|^6\rangle}{\langle\|\psi(\omega)\|^4\rangle^2} \tag{13}$$

and

$$a_2(\omega)\equiv\frac{\langle\|\psi(\omega)\|^2\rangle^2\langle\|\psi(\omega)\|^8\rangle}{\langle\|\psi(\omega)\|^4\rangle^3}. \tag{14}$$

[Notice that, if the differential scattering cross sections of all scatterers are the same, we have $a_1(\omega)=1$, and $a_2(\omega)=1$.] Similarly

$$b_1(\omega)\equiv\frac{\iiint_{\Delta\Omega}d\mathbf{r}\|J(\mathbf{r},\omega)\|^2\iiint_{\Delta\Omega}d\mathbf{r}\|J(\mathbf{r},\omega)\|^6}{\{\iiint_{\Delta\Omega}d\mathbf{r}\|J(\mathbf{r},\omega)\|^4\}^2} \quad (15)$$

and

$$b_2(\omega)\equiv\frac{\{\iiint_{\Delta\Omega}d\mathbf{r}\|J(\mathbf{r},\omega)\|^2\}^2\iiint_{\Delta\Omega}d\mathbf{r}\|J(\mathbf{r},\omega)\|^8}{\{\iiint_{\Delta\Omega}d\mathbf{r}\|J(\mathbf{r},\omega)\|^4\}^3} \quad (16)$$

are related to the transducer-pulser-receiver system.

Using Eqs. (10)–(12), we can simplify Eq. (7), obtaining

$$\sigma_\Lambda^2\approx\frac{1}{n}\left\{4+\frac{22}{M_{\text{eff}}(\omega)}+\frac{5+8a_1(\omega)b_1(\omega)}{M_{\text{eff}}^2(\omega)}+\frac{4-4a_1(\omega)b_1(\omega)+a_2(\omega)b_2(\omega)}{M_{\text{eff}}^3(\omega)}\right\} \quad (17)$$

and

$$\frac{\sigma_\Lambda}{\Lambda(\omega)}\approx\left[\frac{1}{n}\left(4M_{\text{eff}}^2(\omega)+22M_{\text{eff}}(\omega)+5+8a_1(\omega)b_1(\omega)+\frac{4-4a_1(\omega)b_1(\omega)+a_2(\omega)b_2(\omega)}{M_{\text{eff}}(\omega)}\right)\right]^{1/2}. \quad (18)$$

We obtain the scatterer number density by fitting the experimental determinations of $\Lambda(\omega)$ versus frequency to a third-order polynomial over the transducer bandwidth and using the resultant curve to compute $N_{\text{eff}}(\omega)$ at the center frequency, ω_0 of the transducer; i.e., calling $\Lambda(\omega_0)$ the curve-fitted value of $\Lambda(\omega)$ at ω_0, from Eq. (5) we have

$$N_{\text{eff}}(\omega_0)\approx\underline{\Lambda(\omega_0)}^{-1}\times\frac{\iiint_{\Delta\Omega}d\mathbf{r}\|J(\mathbf{r},\omega_0)\|^4}{\{\iiint_{\Delta\Omega}d\mathbf{r}\|J(\mathbf{r},\omega_0)\|^2\}^2}. \quad (19)$$

Assuming that the relative standard error (relative standard deviation of the mean) in $\Lambda(\omega)$ is sufficiently frequency independent over the range of frequencies involved, the relative standard error in the effective scatterer number density is given by

$$\frac{\sigma_{N_{\text{eff}}}}{\Lambda_{N_{\text{eff}}}(\omega_0)}=\frac{1}{m^{1/2}}\frac{\sigma_\Lambda(\omega_0)}{\Lambda(\omega_0)}=\left[\frac{1}{nm}\left(4M_{\text{eff}}^2(\omega_0)+22M_{\text{eff}}(\omega_0)+5+8a_1(\omega_0)b_1(\omega_0)+\frac{4-4a_1(\omega_0)b_1(\omega_0)+a_2(\omega_0)b_2(\omega_0)}{M_{\text{eff}}(\omega_0)}\right)\right]^{1/2}, \quad (20)$$

where m is the number of independent frequency components over the frequency band used in this average[10] and ω_0 is the center frequency of the transducer.

Equation (20) is somewhat similar to the results given by Sleefe and Lele,[3] though the coefficients of M_{eff} are not the same. The latter authors' derivation involved expanding their computed probability density function for the scatterer number density in a Taylor series in terms of the number of scatterers and retaining the first two terms. They model the scatterers as a set of reflectors with reflection coefficients having a zero-mean Gaussian distribution and assume the ultrasonic system has a Gaussian weighted sinusoid impulse response and a beam collimated at −3 dB. Although the approach followed by Sleefe and Lele differs considerably from ours, it is of interest that the predicted relative standard deviation has a similar functional dependence on M_{eff}.

TABLE I. The frequency dependent coefficients, $a_1(\omega)$ and $a_2(\omega)$, for the phantoms. These parameters are calculated using Eqs. (13) and (14).

	3.5 MHz	5.0 MHz
$a_1(\omega)$	1.04	1.03
$a_2(\omega)$	1.13	1.09

II. COMPARISONS WITH EXPERIMENTAL RESULTS

A. Experimental technique

Three phantoms were used to test the expressions for the uncertainty of the experimentally determined effective scatterer number density. The phantoms consist of agar cylinders, 9.0 cm in diameter and 6.0 cm long, with 50-μm-thick Saran Wrap™ windows to allow transmission of ultrasound waves. Embedded in the agar are randomly positioned glass spheres, which have a mean diameter of 73 μm with a standard deviation of 5 μm. The diameter distribution of the glass beads is the same in all three phantoms; however, the scatterer concentration (number per unit volume) is different, viz., 134, 400, and 750 cm^{-3}. The magnitude of the angular distribution function, $\|\psi_i(\omega)\|$ was computed for the different diameter scatterers using the physical properties of the glass beads and equations of Faran.[11] Using these values, the size distribution, and Eqs. (13) and (14), the parameters $a_1(\omega)$ and $a_2(\omega)$ were computed for the phantoms. These are listed in Table I for frequencies relevant to the present work. The ultrasonic speed in each phantom is 1555 m/s while the attenuation coefficient is small over the 1–6 MHz range being, for example, 0.612 dB/cm at 3 MHz.

Either of two focused transducers were used to transmit pulses and receive the resulting backscattered echo signals. One is 3.5 MHz, has a 19.2-mm aperture and a radius of curvature (ROC) of 9.65 cm. The other is 5 MHz with an 18.6-mm aperture and an 8.5 cm ROC. The transducers were driven by one cycle voltage pulses, whose central frequency was the same as the nominal frequency specified by the manufacturer. The phantoms were placed near the focal region of the transducer, and echo signal waveforms were recorded with a LeCroy 9400 digital oscilloscope. The 396 independent echo signals were obtained for each phantom by translating the transducer perpendicular to the sound beam axis. At the end of each experiment, the echo signal from a planar reflector was recorded, from which the product $T(\omega)B_0(\omega)$ was determined using previously described methods.[12]

All analysis was done using programs written in FORTRAN. The data were analyzed in either 10 or 5 μs segments using software defined rectangular time gates; the two

TABLE II. The instrument dependent factors $b_1(\omega)$ and $b_2(\omega)$, calculated using Eqs. (15) and (16).

Transducer	3.5 MHz (Aperture=19.2 mm, ROC=9.65 cm)	5.0 MHz (Aperture=18.6 mm, ROC=8.50 cm)
Gate duration τ=10 μs	$b_1(\omega)$=1.32 $b_2(\omega)$=1.99	$b_1(\omega)$=1.33 $b_2(\omega)$=2.01
Gate duration τ=5 μs	$b_1(\omega)$=1.32 $b_2(\omega)$=1.98	$b_1(\omega)$=1.32 $b_2(\omega)$=1.97

gate durations yielded two effective volumes [Eq. (9)] for each experiment. $V_g(\omega)$ were computed using an FFT algorithm applied to each gated echo signal. The instrument dependent factors $b_1(\omega)$ and $b_2(\omega)$ were evaluated via numerical integration using Eqs. (15) and (16). Spatial integration in the lateral direction extended beyond the second sidelobe in the beam pattern. These results are given in Table II for both gate durations and transducers. The fact that the $b_1(\omega)$ and $b_2(\omega)$ pair is nearly the same for each transducer-time gate set may be attributed to the fact that the beam shapes are very similar for these focused spherical cap transducers.

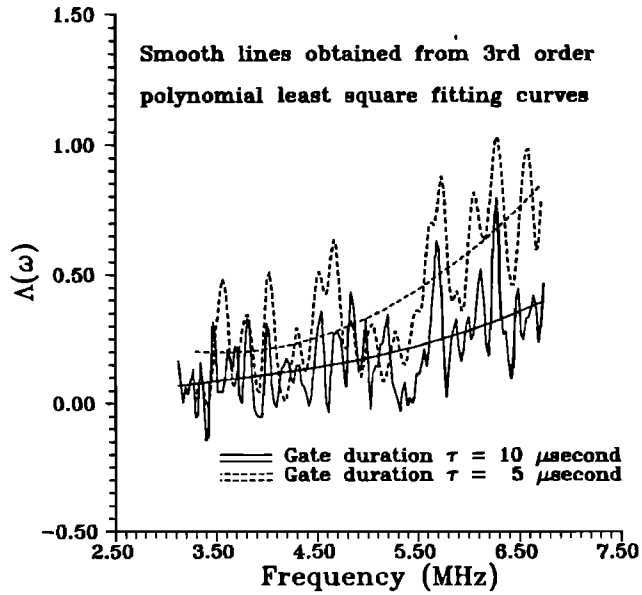

FIG. 2. Typical experimental results of $\Lambda(\omega)$ versus ultrasonic frequency and their polynomial fitting curves. Results for gate durations of 10 and 5 μs are presented. A 5-MHz focused transducer and a 400/cm^3 phantom were used.

B. Results

$I_n(\omega)$ and $J_n(\omega)$ were computed using the Fourier transformed echo data, n always being 396. Values of $\Lambda(\omega)$ were then obtained over a range of frequencies around the center frequency of the transducer. In Fig. 2 are shown graphs of $\Lambda(\omega)$ versus frequency for the 400 cm^{-3} phantom and the 5-MHz center frequency transducer; one set of data corresponds to a 5-μs time gate and the other to a 10-μs time gate. The smooth curves in Fig. 2 were obtained by fitting the data to third-order polynomials. As mentioned previously, the value of the fitted curve at the transducer center frequency is used as an estimator for $Y(\omega_0)$ in Eq. (5), yielding the effective number density $N_{\text{eff}}(\omega_0)$.

In Table III are shown comparisons of the theoretical predictions and experimental results of the variance of $\Lambda(\omega)$. Columns 2, 3, and 4 are for the 3.5-MHz transducer, while columns 5, 6, and 7 are for the 5-MHz transducer. The actual scatterer concentration in each phantom is presented in the second row. Effective scatterer number densities computed using Eq. (3) are given in row 3 for each phantom. The effective sample volume [Eq. (9)] was calculated for each gate duration, and is listed in row 4 for the 5-μs time gate and row 8 for the 10-μs gate. The product of the effective scatterer number density $N_{\text{eff}}(\omega)$ and the effective sample volume $V_{\text{eff}}(\omega)$ yields $M_{\text{eff}}(\omega)$, the average effective number of scatterers contributing to the gated signal waveforms. These values are presented in rows 5 and 9. For example, for a 5 μs gate duration, $M_{\text{eff}}(\omega)$ ranged from 0.96 for the 134 cm^{-3} phantom studied using the 5-MHz transducer to 14.88 for the 750-cm^{-3} phantom and the 3.5-MHz transducer. When a 10-μs time gate is applied, $M_{\text{eff}}(\omega)$ increases correspondingly as shown in row 9. The theoretical predictions of

TABLE III. Comparisons of the theoretical prediction and the experimental results of the variance of the ratio of the fourth moment to the square of the second moment of the echo signal. Comparisons were done both at 3.5 and 5 MHz for all three phantoms.

Ultrasound frequency (MHz)		3.5			5.0		
Scatterer concentration $\langle N\rangle$ (cm^3)		134	400	750	134	400	750
$N_{\text{eff}}(\omega)$ (mm^{-3})		0.129	0.386	0.724	0.129	0.386	0.724
	$V_{\text{eff}}(\omega)$ (mm^{-3})	20.40	20.54	20.56	7.44	7.63	7.29
τ=5	$M_{\text{eff}}(\omega)$	2.63	7.93	14.88	0.96	2.94	5.28
(μs)	$\sigma^2_{\Lambda\text{theory}}$	0.0372	0.0178	0.0140	0.114	0.0337	0.0209
	$\sigma^2_{\Lambda\text{experiment}}$	0.0402	0.0139	0.0135	0.142	0.0330	0.0228
	$V_{\text{eff}}(\omega)$ (mm^{-3})	42.88	43.05	43.11	15.94	16.08	15.99
τ=10	$M_{\text{eff}}(\omega)$	5.53	16.62	31.21	2.06	6.21	11.58
(μs)	$\sigma^2_{\Lambda\text{theory}}$	0.0215	0.0134	0.0119	0.0467	0.0201	0.0152
	$\sigma^2_{\Lambda\text{experiment}}$	0.0257	0.0125	0.0190	0.0518	0.0209	0.0187

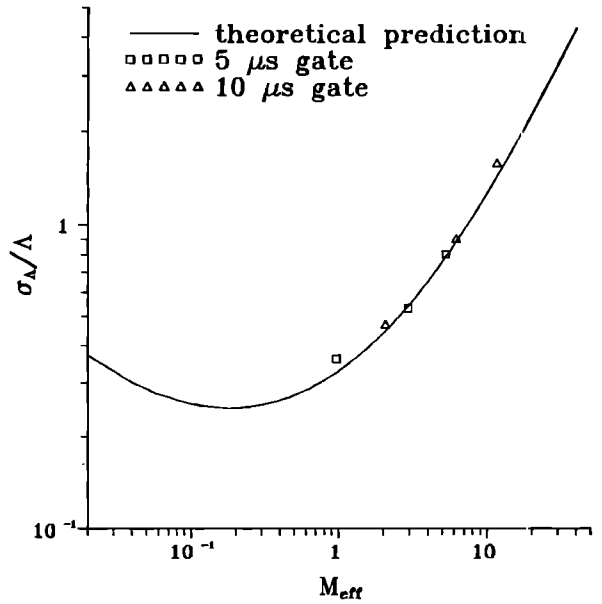

FIG. 3. The experimental results and theoretical predictions of relative standard deviations of the variable $\Lambda(\omega)$ when a 5-MHz transducer was used.

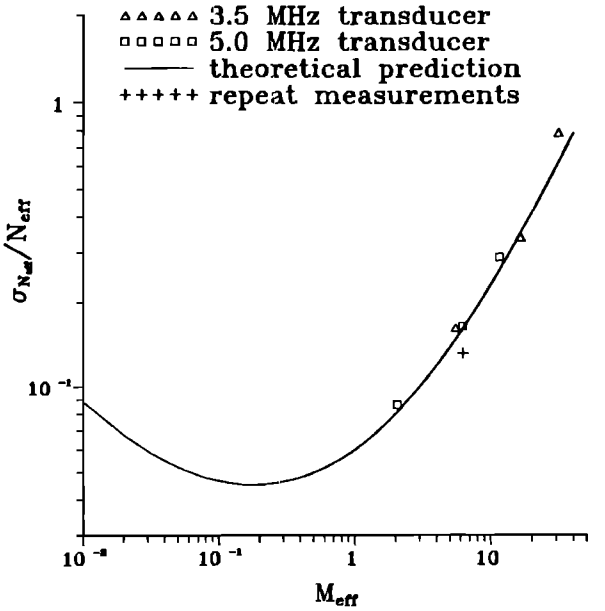

FIG. 5. The experimental and theoretical results for the relative standard error (relative standard deviation of the mean) of the effective scatterer number density estimation when a 10-μs time gate was used.

the variance of Λ based on Eq. (17), $\sigma^2_{\Lambda|\text{theory}}$, are shown in rows 6 and 10, while the experimental results, $\sigma^2_{\Lambda|\text{experiment}}$ are shown in rows 7 and 11. The latter results were determined using the mean square deviation of $\Lambda(\omega)$ from the polynomial fit where it has been assumed that σ^2_Λ does not vary significantly over the bandwidth of the transducer. As can be seen, the experimental results are in reasonably good agreement with the results computed using Eq. (17).

The relative standard deviation of $\Lambda(\omega_0)$ depends on $M_{\text{eff}}(\omega)$, the effective number of scatterers contributing to the truncated echo signal. This is shown in Figs. 3 and 4 for the 5- and 3.5-MHz transducer data, respectively. Each data point shows results from one of the three phantoms evaluated using either the 5- or the 10-μs time gate. In computing the

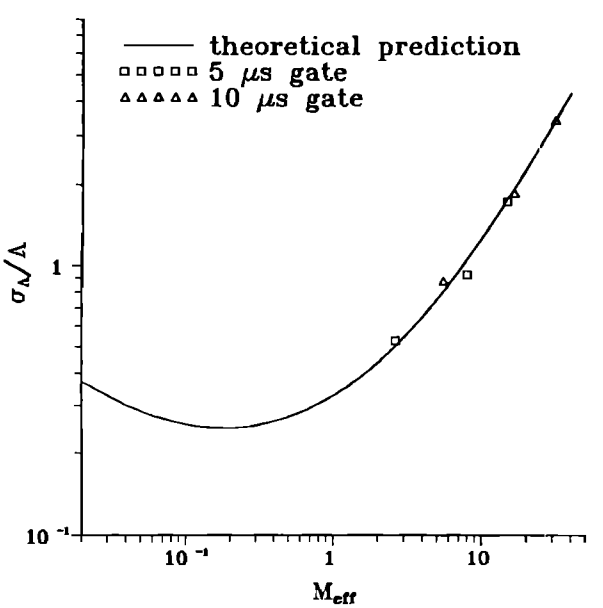

FIG. 4. The experimental results and theoretical predictions of relative standard deviations of the variable $\Lambda(\omega)$ when a 3.5-MHz transducer was used.

experimental value of $\sigma_\Lambda(\omega_0)/\Lambda(\omega_0)$, we used $\Lambda(\omega_0) = \Lambda(\omega_0)$, the curve-fitted value at the transducer center frequency. Solid lines in the figures are the theoretical predictions obtained by evaluating Eq. (18). These appear to be in good agreement with experimental values. The fact that the relative standard deviation becomes greater when the average effective number of scatterers is increased has also been noted by previous researchers.[3]

The relative standard deviations for the $N_{\text{eff}}(\omega)$ estimates are lower than those shown in Figs. 3 and 4 because the polynomial fit is over a range of frequencies. The number of independent frequency components contributing to the fit, m, may be estimated from the ultrasound pulse bandwidth and the bandwidth of the time gate used to truncate the echo signal.[10] For example, if a T-μs time gate is used, the frequency bandwidth for each independent frequency component will be on the order of $1/T$ MHz; the number of independent frequency components will, therefore, be $m \approx BT$ for an ultrasound frequency band of B MHz. Thus, for each transducer, the number of independent frequency components is $m \approx 30$ for the 10-μs gate duration ($B=3$ MHz; $1/T=0.1$ MHz), and ≈ 15 for the 5-μs gate.

Figures 5 and 6 show relative standard deviations of the mean (relative standard errors) of the effective scatterer number density when the number of frequency components m is taken into account. Equation (20) was used to compute the smooth curves, while the data points are the mean square deviations of the experimental data points from the smooth curves.

The two additional data points (+) in Figs. 5 and 6 are relative standard deviations obtained from repeated measurements of $N_{\text{eff}}(\omega_0)$ in the 400 cm ^{3} phantom. Six sets of measurements were obtained using the 5-MHz transducer. Table IV lists the results of each measurement set, both for a 5- and a 10-μs time gate applied during the analysis. The relative

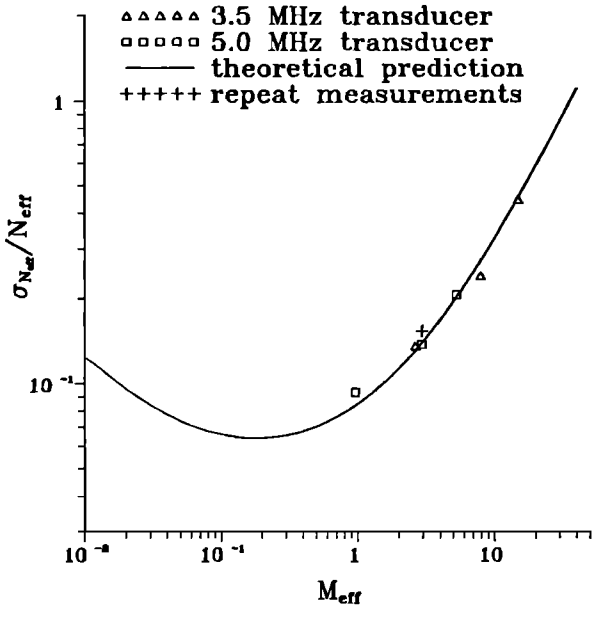

FIG. 6. The experimental and theoretical results for the relative standard error (relative standard deviation of the mean) in the effective scatterer density estimation when a 5-μs time gate was used.

standard deviations obtained for repeat measurements appear to correspond well with the relative standard error calculations derived from the statistical fluctuations in the data from a single measurement (□'s and △'s) as well as predictions based on the error analysis (solid line in Figs. 5 and 6). Both experimental and predicted results are also in agreement regarding the large error when $M_{eff}(\omega)$ is greater than 8–10.

III. DISCUSSION

An expression for the statistical uncertainty of the effective scatterer number density determined from ultrasound pulse-echo data has been derived. The relative standard error [Eq. (20)] depends mainly on the number of statistically independent echo signals obtained from the volume of interest, the number of independent frequency components involved in the estimate and $M_{eff}(\omega)$, the average effective number of scatterers contributing to each echo signal waveform. The predicted statistical uncertainty agrees both with uncertainties based on fluctuations in echo signal data for a given measurement of $N_{eff}(\omega)$ and with standard deviations for results of repeat measurements of $N_{eff}(\omega)$ in phantoms.

TABLE IV. Results of six different measurements of the effective scatterer number density in the 400 cm^{-4} phantom.

Experiment number	5-μs gate	10-μs gate
1	462 cm^{-3}	445 cm^{-3}
2	353 cm^{-3}	380 cm^{-3}
3	303 cm^{-3}	302 cm^{-3}
4	333 cm^{-3}	338 cm^{-3}
5	406 cm^{-3}	369 cm^{-3}
6	355 cm^{-3}	359 cm^{-3}
Mean±s.d.	369±57 cm^{-3}	366±48 cm^{-3}

When the number of scatterers within the effective sample volume is large (i.e., greater than 10), the statistical properties of the echo signal approach those of a Rayleigh distribution.[13] The ratio of the fourth moment to the square of the second moment in Eq. (10) goes to two, and information on the scatterer number density is lost. This is exhibited in the present paper by the very large statistical errors when the number of scatterers contributing to the signal (M_{eff}) goes beyond 10. The most useful application of the method would appear to be for measuring number densities in the "just unresolvable," i.e., in the 1 to 10 per effective sample volume range. This general conclusion has been stated previously by Wagner *et al.*[14] who note that only for small numbers, say 2–3 per "speckle cell" are reasonable results obtained using these methods.

In general, reducing the effective sample volume reduces $M_{eff}(\omega)$ and hence the uncertainty in the number density estimator. This trend is easily seen in the data, where dependencies of the error on ultrasound transducer frequency and duration of the time gate used to select a region of interest are apparent—and are accurately predicted. Thus to the extent possible with the sample, the experimental conditions (beam focusing, gate duration, number of echo signal waveforms) could be optimized to reduce the statistical error as low as practical. An important aspect of the present work is that effects of various experimental parameters on the accuracy of the result, including transducer geometric parameters, transducer frequency bandwidth, and the analysis time gate may be predicted.

In any measurement, systematic errors as outlined in the introduction must also be considered in making a final estimation of the effective scatterer number uncertainty. Usually these can be minimized by careful calibrations of the measurement system and by understanding the properties of the medium.

ACKNOWLEDGMENTS

This work was supported in part by NIH grant R01-CA39224 and by a UW Medical Physics, Richard B. Mazess Advanced Fellowship.

[1] J. F. Chen, E. L. Madsen, and J. A. Zagzebski, "A method for determination of frequency dependent effective scatterer number density," J. Acoust. Soc. Am. **95**, 77–85 (1994).
[2] L. X. Yao, J. A. Zagzebski, and E. L. Madsen, "Statistical uncertainty in ultrasonic backscatter and attenuation coefficients determined with a reference phantom," Ultrasound Med. Biol. **17**, 187–193 (1991).
[3] G. E. Sleefe and P. P. Lele, "On estimating the number density of random scatterers from backscattered acoustic signals," Ultrasound Med. Biol. **14**, 709–729 (1988).
[4] G. E. Sleefe and P. P. Lele, "Tissue characterization based on scatterer number density estimation," IEEE Trans. Sonics Ultrason. **SU-35**, 749–757 (1988).
[5] P. Wihelmij and P. Denbigh, "A statistical approach to determining the number density of random scatterers from backscattered pulses," J. Acoust. Soc. Am. **76**, 530–540 (1984).
[6] P. Denbigh and Q. Smith, "Determination of fish number density by a statistical analysis of backscattered sound," J. Acoust. Soc. Am. **90**, 457–469 (1991).
[7] P. M. Morse and K. U. Ingard, *Theoretical Acoustics* (McGraw-Hill, New York, 1968), Chap. 8.

[8] E. Jakeman, "Speckle statistics with a small number of scatterers," Opt. Eng. **24**, 453–461 (1984).
[9] P. B. Bevington, *Data Reduction and Error Analysis for Physical Science* (McGraw-Hill, New York, 1969).
[10] P. Karpur, P. M. Shankar, J. L. Rose, and V. L. Newhouse, "Split spectrum processing: optimizing the processing parameters using minimization," Ultrasonics **25**, 204–208 (1987).
[11] J. J. Faran, "Sound scattering by solid cylinders and spheres," J. Acoust. Soc. Am. **23**, 405–418 (1951).
[12] E. L. Madsen, M. F. Insana, and J. A. Zagzebski, "Method of data reduction for accurate determination of acoustic backscatter coefficient," J. Acoust. Soc. Am. **76**, 913–923 (1984).
[13] R. F. Wagner, M. F. Insana, and S. W. Smith, "Fundamental correlation lengths of Coherent speckle in medical ultrasonic images," IEEE Trans. Sonics Ultrason. **SU-35**, 749–757 (1988).
[14] R. F. Wagner, D. G. Brown, K. A. Wear, M. F. Insana, and T. J. Hall, "Statistical properties of the scatterer number density estimator," Ultrason. Imag. **13**, 192 (1991).